Desalination and Water Treatment
www.deswater.com

doi: 10.1080/19443994.2012.749019

51 (2013) 2554–2563
March

Taylor & Francis
Taylor & Francis Group

Organic dye adsorption on activated carbon derived from solid waste

A.A. Ahmad[a,*], A. Idris[a], B.H. Hameed[b]

[a]*Faculty of Engineering, Department of Chemical and Environmental Engineering, University Putra Malaysia, 43400 UPM, Serdang, Malaysia*
Tel. +60 3 89466302; Fax: +60 3 86567120; email: abdulbari@eng.upm.edu.my
[b]*School of Chemical Engineering, Engineering Campus, University Science of Malaysia, 14300 Nibong Tebal, Penang, Malaysia*

Received 15 July 2011; Accepted 23 August 2012

ABSTRACT

Activated carbon was prepared through a chemical activation of bamboo waste precursor (BMAC) using phosphoric acid as the activating agent at 500°C for 2 h. Batch adsorption studies were carried out for the adsorption of C.I. Reactive Black 5 (RB5) onto the BMAC. The effect of various experimental parameters such as initial dye concentration (50–500 mg/L), contact time (0–32 h), pH (2–12), and temperature (30–50°C) were investigated. Equilibrium data were found to be very well represented by the Freundlich isotherm and a pseudo-second-order model was found to explain the kinetics of RB5 adsorption more effectively. The mechanism of the adsorption process was determined by the intraparticle diffusion model. Thermodynamic parameters such as standard enthalpy (ΔH°), standard entropy (ΔS°), standard free energy (ΔG°), and activation energy were determined. The results indicated that BMAC is a suitable adsorbent material for adsorption of reactive dye from aqueous solutions.

Keywords: Bamboo waste; Activated carbon; C.I. Reactive Black 5; Isotherm; Kinetics

1. Introduction

Azo dyes are synthetic organic compounds widely used in textile dyeing, paper printing, and other industrial processes such as the manufacture of pharmaceutical drugs, toys, and foods including candies. This class of dyes, which is characterized by the presence of at least one azo bond (–N=N–) bearing aromatic rings, dominates the worldwide market of dyestuffs with a share of about 70% [1]. Reactive dyes are typically azo-based chromophores combined with different types of reactive groups. Reactive dyes posses some peculiar advantages, such as bright colors, excellent colorfastness, and ease of application [2,3]. However, many reactive dyes are toxic to living organisms and exhibiting poor biodegradability tendencies (especially those containing azo-groups) [4]. Moreover, since reactive dyes are highly soluble in water, their removal from effluent is difficult by conventional physicochemical and biological treatment methods [5].

Adsorption onto activated carbon has been found to be superior for removal of pollutants from wastewaters compared to other physical and chemical techniques [6]. Adsorption processes are characterized by kinetics and isotherm. Both isotherm and kinetic data are important tools to understand the mechanism and

*Corresponding author.

design of adsorption treatment plant [7]. Activated carbons is the most widely used adsorbent for the removal of dyes and treatment of textile effluents, because of their exceptionally large surface areas, well-developed internal pore structure as well as their surface reactivity attributed to the existence of a wide spectrum of oxygen containing surface groups [8,9]. In the past few years, extensive research has been undertaken to develop alternative and economic adsorbents. An economic adsorbent is defined as one which is abundant in nature, or is a by-product or waste from industry, that has little or no economic value and requires little processing [10]. Several million tons of agricultural wastes are being disposed in the world every year through different ways such as incineration, land applications, and land filling. Agricultural residues, known as lignocellulosic biomass resources, are defined as a biomass by-product from the agricultural system includes straws, husks, shells, fruit stones, and stalks [10].

Bamboo is an abundant natural resource in Malaysia because it takes only several months to grow up. It has been traditionally used to construct various living facilities and tools [11]. Bamboo has been used as the structural material for steps at construction sites in China, India, Malaysia, and other countries because it is a strong, tough, and low-cost material. Conversion of bamboo waste to a value-added product such as activated carbon will help to solve part of the problem of wastewater treatment in Malaysia.

Therefore, the purpose of this work was to evaluate the adsorption potential of bamboo-based activated carbon for C.I. Reactive Black 5. The equilibrium, kinetic, and thermodynamic data of the adsorption process were then studied to understand the adsorption mechanism of RB5 molecules onto the prepared activated carbon.

2. Theoretical background

2.1. Equilibrium modeling

The analysis of the isotherm data by fitting them to different isotherm models is an important step to find the suitable model that can be used for design purposes [12].

The Langmuir equation is valid for monolayer adsorption on a surface with a finite number of identical sites and is expressed as [13]:

$$q_e = \frac{q_m K_L C_e}{1 + K_L C_e} \tag{1}$$

The linear expression of the Langmuir model is given by Eq. (2):

$$\frac{C_e}{q_e} = \frac{1}{Q_o b} + \frac{1}{Q_o} C_e \tag{2}$$

where C_e (mg/L) is the initial concentration of adsorbate and q_e (mg/g) is the amount of adsorbate adsorbed per unit mass of adsorbent. Q_o is the maximum amount of the dye per unit mass of adsorbent to form a complete monolayer on the surface at high C_e (mg/L) and b (L/mg) is a constant related to the affinity of the binding sites.

The essential characteristics of the Langmuir isotherm can be expressed in terms of a dimensionless equilibrium parameter (R_L) [14], which is defined by:

$$R_L = \frac{1}{(1 + bC_o)} \tag{3}$$

where C_o (mg/L) is the initial amount of adsorbate and b (L/mg) is the Langmuir constant described above. There are four probabilities for the R_L value: (i) for favorable adsorption $0 < R_L < 1$, (ii) for unfavorable adsorption $R_L > 1$, (iii) for linear adsorption $R_L = 1$, and (iv) for irreversible adsorption $R_L = 0$.

The empirical Freundlich isotherm [15] based on adsorption on a heterogeneous surface is given by the following equation:

$$q_e = K_F C_e^{1/n} \tag{4}$$

A linear form of the Freundlich expression can be obtained by taking logarithms of the following equation:

$$\log q_e = \log K_F + \frac{1}{n} \log C_e \tag{5}$$

where K_F (mg/g (L/mg)$^{1/n}$) and n are Freundlich constants with n giving an indication of how favorable is the adsorption process. K_F is the adsorption capacity of the adsorbent which can be defined as the adsorption or distribution coefficient and represents the quantity of dye adsorbed onto activated carbon for a unit equilibrium concentration. The slope of $1/n$ ranging between 0 and 1 is a measure of adsorption intensity or surface heterogeneity, becoming more heterogeneous as its value gets closer to zero [16]. Value for $1/n$ below one indicates a normal Langmuir isotherm while $1/n$ above one is an indicator for cooperative adsorption [17].

Temkin isotherm [18] contains a factor that explicitly takes into account of adsorbing species–adsorbate interactions. The Temkin isotherm is represented by the following equation:

$$q_e = RT/b \ln(K_t C_e) \tag{6}$$

Eq. (6) can be expressed in its linear form as

$$q_e = B \ln K_t + B \ln C_e \quad (7)$$

where

$$B = RT/b \quad (8)$$

The adsorption data can be analyzed according to Eq. (5). A plot of q_e vs. $\ln C_e$ enables the determination of the isotherm constants K_t and B. K_t (L/mg) is the equilibrium binding constant corresponding to the maximum binding energy and constant B is related to the heat of adsorption.

2.2. Kinetics of adsorption

In order to examine the controlling mechanism of adsorption processes such as mass transfer, equilibrium time, and chemical reaction, several kinetic models were used to test experimental data. The pseudo-first-order and pseudo-second-order kinetic models were applied to study the kinetics of the adsorption process. The pseudo-first-order rate expression of Lagergren [19] is:

$$\log(q_e - q_t) = \log q_e - \frac{k_1}{2.303} t \quad (9)$$

where q_e and q_t (mg/g) are the amounts of RB5 adsorbed at equilibrium and at time t (h), respectively and k_1 (h^{-1}) is the adsorption rate constant. A straight line of log $(q_e - q_t)$ vs. t would suggest the applicability of this kinetic model.

The pseudo-second-order [20] equation based on equilibrium adsorption data is expressed as:

$$\frac{t}{q_t} = \frac{1}{k_2 q_e^2} + \frac{1}{q_e} t \quad (10)$$

where k_2 (g/mg h) is the rate constant for the pseudo-second-order adsorption kinetics.

2.3. Validity of kinetic model

The applicability of the kinetic model to describe the adsorption process was further validated by the normalized standard deviation Δq (%) which is defined as [21]:

$$\Delta q(\%) = 100 \sqrt{\frac{\sum [(q_{\exp} - q_{\text{cal}})/q_{\exp}]^2}{N - 1}} \quad (11)$$

where N is the number of data points, $q_{\exp}$ and q_{cal} (mg/g) are the experimental and calculated adsorption capacity, respectively.

2.4. Intraparticle diffusion

Intraparticle diffusion model based on the theory proposed by Weber and Morris [22] was tested to identify the diffusion mechanism. Adsorption is a multistep process involving transport of the solute molecules from the aqueous phase to the surface of the solid particulates followed by diffusion into the interior of the pores. According to this theory:

$$q_t = K_i t^{1/2} + C \quad (12)$$

where k_i (mg/g $h^{1/2}$), the intraparticle diffusion rate constant, is obtained from the slope of the straight line of q_t vs. $t^{1/2}$.

2.5. Adsorption thermodynamics

The concept of thermodynamic assumes that in an isolated system where energy cannot be gained or lost, the entropy change is the driving force [23]. The thermodynamic parameters that must be considered to determine the process are changes in standard enthalpy (ΔH°), standard entropy (ΔS°), and standard free energy (ΔG°) due to transfer of unit mole of solute from solution onto the solid–liquid interface. The value of ΔH° and ΔS° were computed using the following equation:

$$\ln K_c = \frac{\Delta S^o}{R} - \frac{\Delta H^o}{\text{RT}} \quad (13)$$

where R (8.314 J/mol K) is the universal gas constant, T (K) the absolute solution temperature, and K_c is the distribution coefficient which can be calculated as:

$$K_c = \frac{q_e}{C_e} \quad (14)$$

The values of ΔH° and ΔS° were calculated from the slope and intercept of plot between $\ln K_c$ vs. $1/T$. ΔG° can be calculated using the relation below:

$$\Delta G_{\text{ads}} = \Delta H_{\text{ads}} - T\Delta S_{\text{ads}} \quad (15)$$

3. Materials and methods

3.1. Adsorbate

C.I. Reactive Black 5 (RB5), diazenyl-3-[[4-(2-sulfonatooxyethylsulfonyl)phenyl] hydrazinylidene]

naphthalene-2,7-disulfonate supplied by Sigma–Aldrich (M) Sdn Bhd, Malaysia was used as an adsorbate without any further purification. Distilled water was used to prepare all solutions. RB5 has a chemical formula of $C_{26}H_{21}N_5Na_4O_{19}S_6$, with molecular weight of 991.82 g/mol. The chemical structure of C.I. Reactive Black 5 (RB5) is shown in Fig. 1.

3.2. Activated carbon preparation

Bamboo waste was collected from a local furniture shop, Penang State, Malaysia. The procedure used to prepare the activated carbon was referred to our previous work [24]. It was washed with hot distilled water to remove dust like impurities then dried in an oven (Model Memmert 600, Germany) at temperature of 105°C for 24 h and thereafter crushed and sieved to the desired particle size range (200–300 μm). Chemical activation method using phosphoric acid (purity 85% Merck, Germany) was used to activate the raw material. In a typical batch production, 40 g of raw material was impregnated by certain amount of 40 wt.% concentrated phosphoric acid with occasional stirring. The amount of phosphoric acid solution used was adjusted to give a certain impregnation ratio. Subsequently, the impregnated samples were air dried under sunlight for three days. Activation of phosphoric acid impregnated precursor was carried out at a temperature of 500°C (at a heating rate of 10°C/min) for 2 h under nitrogen flow rate at 150 cm^3/g and. After activation, the samples were allowed to cool down under the nitrogen environment. The samples were subsequently washed several times with hot distilled water (70°C) until the pH of the washing solution reached 6–7. Finally samples were dried in an oven at 110°C for 24 h and then stored in plastic containers.

Textural characterization of the BMAC was carried out by N_2 adsorption at 77 K using ASAP 2020 Micromeritics instrument by Brunauer–Emmett–Teller (BET) method, using the software of Micromeritics. Surface morphology and the presence of porosity of the activated carbon prepared in this work were studied using scanning electron microscopy (SEM) analysis.

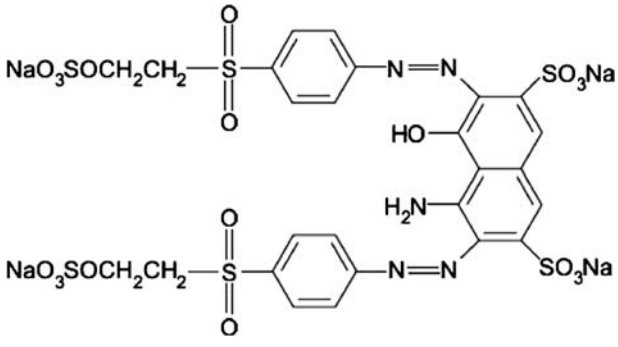

Fig. 1. Chemical structure of C.I. Reactive Black 5 (RB5).

3.3. Chemical characteristics of activated carbon

The surface chemistry characterization of the prepared activated carbon was performed with pH drift method. pH_{PZC} (point of zero charge) is pH when the charge in the activated carbon surface is zero. For this purpose, 50 ml of 0.01 N NaCl were prepared and added into a series of Erlenmeyer. Then, their pH values were adjusted in range between 2 and 12 with interval 0.1 using 0.01 N HCl solutions and 0.01 N NaOH. pH of initial solutions were measured with pH meter and then noted as $pH_{initial}$. After constant value of $pH_{initial}$ had been reached, 0.15 g of activated carbon sample was added into each Erlenmeyer and then shaken for 48 h. After 48 h, pH of solution was measured using pH meter and noted as pH_{final}. pH_{PZC} of activated carbon sample is the point when $pH_{initial} = pH_{final}$.

The functional groups available on the surface of the prepared activated carbon were detected by KBr technique using a Fourier Transform Infrared (FTIR) spectroscope (FTIR-2000, PerkinElmer). The spectra were recorded from 4000 to 400 cm^{-1}.

3.4. Equilibrium studies

Adsorption experiments were carried out by adding a fixed amount of adsorbent (0.30 g) to a series of 250 mL conical flasks filled with 200 mL diluted dye solutions (50–500 mg/L). The conical flasks were then sealed and placed in a water bath shaker and the agitation speed set at 120 rpm. The water bath temperatures of 30, 40, and 50°C were investigated. At the end of each adsorption batch runs, the final concentration of RB5 in the solution was measured at 597 nm using UV/Vis spectrophotometer (Shimadzu UV/Vis 1601 Spectrophotometer, Japan). Before the measurement was made, a calibration curve was plotted using the standard RB5 with known concentrations. The amount of dye on BMAC adsorbent was calculated from the following equation:

$$q_e = \frac{(C_o - C_e)V}{W} \tag{16}$$

where q_e (mg/g) is the amount of dye adsorbed at equilibrium, C_o and C_e (mg/L) are the liquid-phase concentrations of dye at initial and equilibrium points respectively. V (L) is the volume of the solution and W (g) is the mass of dry adsorbent used.

3.5. Effect of solution pH and temperatures

To study the effect of solution pH on the removal of dye by BMAC adsorbent, the pH was adjusted by adding a few drops of 0.1 M NaOH and 0.1 M HCl before each run. Experimental conditions were 0.30 g BMAC; 200 mg/L dye solution, temperature equal to 30 ℃, and contact time of 24 h. The effect of temperature 30, 40, and 50 ℃ on the adsorption on BMAC was studied using initial dye concentrations of 50–500 mg/L for 24 h and pH values ranging between 2 and 12.

4. Results and discussion

4.1. BET and SEM of the activated carbon

The BET surface area, Langmuir surface area, total pore volume, and average pore diameter of the prepared activated carbon were 988.23 m^2/g, 1561.164 m^2/g, 0.696 cm^3/g, and 2.82 nm, respectively. The SEM image of the derived activated carbon was referred to our previous work [25]. Many large pores in a honeycomb shape were clearly found on the surface of the activated carbon. The well-developed pores had led to the large surface area and porous structure of the activated carbon.

4.2. Chemical characteristics of activated carbon

The pH_{PZC} value was obtained for the prepared activated carbon was around 5.5 ± 3, indicating that the surface of the activated carbon was more on the acidic groups. This was in agreement with the work carried out by Hamdaoui and Naffrechoux [26] and Prahas et al. [27] which reported that the surface of activated carbon was as well showing acidic characteristic. The FTIR spectrum of the prepared activated carbon was referred to our previous work [25]. The spectrum displayed the following bands:

3736 cm^{-1}: O–H stretching vibrations;
2373 cm^{-1}: C≡O stretching vibrations;
1538 cm^{-1}: C=C stretching vibration in aromatic rings;
1052 cm^{-1}: C–OH stretching vibrations;
674 cm^{-1}: C–H out-of-plane bending in benzene derivatives.

The main surface functional groups present in the derived activated carbon were quinone and aromatic rings.

4.3. Effect of initial dye concentrations

Fig. 2 shows the effects of agitation time and initial dye concentrations on the adsorption kinetics of BMAC adsorbent at 30 ℃. The adsorption curves are smooth and continuous leading to saturation. An increase in the initial dye concentrations leads to an increase in the adsorption capacity of the dye on BMAC adsorbent. The maximum monolayer adsorption capacity at equilibrium (q_e) increased from 31.25 to 157.54 mg/g with an increase in the initial dye concentrations from 50 to 500 mg/L. Similar behaviors were reported for the adsorption of C.I. reactive orange 12 on coir pith activated carbon [28] adsorption of C.I. acid blue 92 on activated carbon [29] and the adsorption of C.I. Reactive Black 5 on activated sludge [30]. The amount of RB5 adsorbed at the equilibrium time reflected the maximum adsorption uptake of the adsorbent under the operating conditions applied. This was due to the increase in the driving force, the concentration gradient. The high adsorption rate at the beginning of adsorption was likely due to the adsorption of RB5 by the exterior surface of the adsorbent. When saturation was reached at the exterior surface, the RB5 molecules began to diffuse through the pores to the interior surfaces of the particles [31]. Adsorption rate might vary as it depends on several parameters such as stirring rate, structural properties of adsorbent, adsorbent dosage, and adsorbate properties. Fig. 2 also shows that most of the dye was adsorbed to achieve a near adsorption equilibrium within the first 10 h of contact between the adsorbate and the adsorbent. However, the experimental data were measured at 32 h to make sure that full equilibrium was attained. As can be seen from Fig. 2, the amount of RB5 adsorbed on the activated carbon increases with time and, at some point in time, it reaches a constant value beyond which no more RB5 is further removed from the solution.

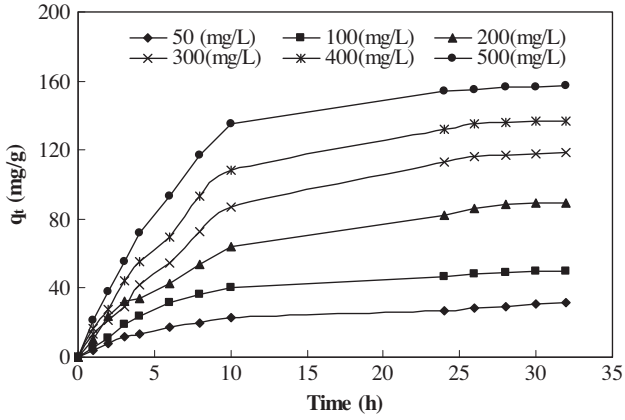

Fig. 2. The variation of adsorption capacities with adsorption time at various initial RB5 concentrations at 30 ℃.

4.4. Effect of solution pH

Fig. 3 shows the effect of solution pH on the removal of RB5 by the prepared activated carbon. As can be seen in Fig. 3, the RB5 removal was found to decrease significantly with an increase in initial pH of the solution from pH 2 to 12. In this study, the highest RB5 removal was achieved at pH 2–6 with RB5 removal as high as 91.72 mg/g. This was due to the chemical characteristics of the activated carbon with acidic pH_{PZC}, which was around 5.5 ± 3. At a solution pH lower than the pH_{PZC}, the total surface charge would be on average positive, whereas at a higher solution pH, it would be negative. A lower adsorption at higher pH values may be due to the abundance of OH^- ions and because of ionic repulsion between the negatively charged surface and the anionic dye molecules. There are also no more exchangeable anions on the outer surface of the adsorbent at higher pH values and consequently the adsorption decreases. At lower pH, more protons will be available, thereby increasing electrostatic attraction between positively charged adsorption sites and dye anions causing an increase in adsorption capacity. Similar results were reported for the adsorption of acid yellow 36 on activated carbons prepared from sawdust and ricehusk [7]. The results were in agreement with the finding reported by Santhy and Selvapathy [28] studied the C.I. reactive orange 12, C.I. reactive red 2, and C.I. reactive blue 4 dyes adsorption onto coir pith activated carbon. They reported that the amounts of reactive dyes adsorbed were high at low pH as compared to high pH.

4.5. Effect of temperature

From Table 1, the maximum monolayer adsorption capacity of RB5 onto the prepared activated carbon increased from 169.49 to 212.76 mg/g with an increase in solution temperature from 30 to 50°C, this indicated the endothermic nature of the adsorption reaction. Increase in the temperature was known to increase the rate of diffusion of the adsorbate molecules across the external boundary layer and in the internal pores of the adsorbent particle. This is owing to the decrease in the viscosity of the solution [32]. The enhancement in the adsorption capacity might be due to the chemical interaction between the adsorbate and the adsorbent, and the creation of some new adsorption sites or the increased rate of intraparticle diffusion of adsorbate molecules into the pores of the activated carbons at higher temperatures [33]. Senthilkumaar et al. [34] noted similar observations and they suggested that the increase in adsorption capacity with an increase in temperature might be due to the possibility of an increase in the porosity and in the total pore volume of the adsorbent, an increase of number of active sites for the adsorption as well as an increase in the mobility of the adsorbate molecules. The foregoing results are consistent with the findings reported by Netpradit et al. [35] for the adsorption of C.I. reactive red 120, and C.I. reactive red 141 dyes on metal hydroxide sludge.

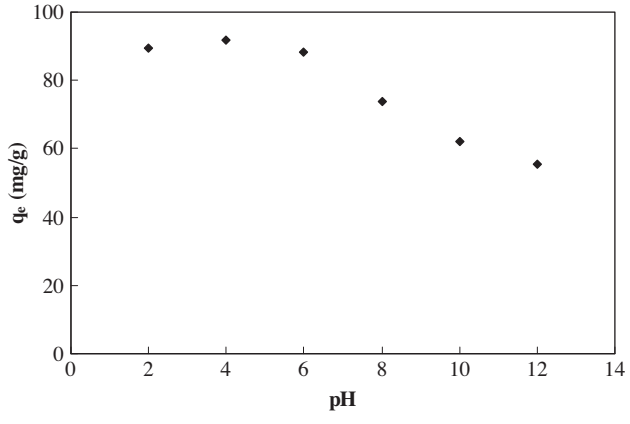

Fig. 3. Effect of pH on the adsorption of RB5 on BMAC at 30°C.

4.6. Adsorption isotherms

The plots of linear form of Langmuir, Freundlich, and Temkin adsorption isotherms of RB5 on BMAC obtained at temperatures of 30–50°C (figure not shown). The correlation coefficients (R^2 values) and the constants obtained from the three isotherm models for the adsorption of RB5 on the BMAC are summarized in Table 1. The maximum monolayer adsorption of the BMAC for removal of RB5 was determined from the Langmuir equation and found to be 169.49, 204.08, and 212.76 mg/g at 30, 40, and 50°C, respectively. The values of R_L calculated from Eq. (2) are listed in Table 1. As the R_L values for all temperatures are between 0 and 1, the adsorption process is favorable. The Freundlich model gave the highest R^2 values which were greater than 0.97 at all the three temperatures studied, showing that the adsorption of RB5 on the BMAC was best described by Freundlich model. This suggested that some heterogeneity on the surfaces or pores of the activated carbon played some significant role in the RB5 adsorption on the BMAC. All the $1/n$ values obtained from the Freundlich model were below one within the investigated solution temperatures, representing that adsorption of RB5 on the BMAC was favorable. From Table 1, the Freundlich isotherm model yielded the best fit with the highest R^2 value at all temperatures compared to the other two models. The order of R^2 was

Table 1
Isotherm parameters and correlation coefficients for adsorption of RB5 on BMAC at different temperatures

Temp. (°C)	Langmuir				Freundlich			Temkin		
	Q_o (mg/g)	b (L/mg)	R^2	R_L	K_F (mg/g(L/mg)$^{1/n}$)	$1/n$	R^2	K_T (L/mg)	B	R^2
30	169.49	0.03	0.96	0.07	20.63	0.38	0.99	11.04	89.16	0.94
40	204.08	0.02	0.93	0.07	26.13	0.35	0.98	6.15	88.59	0.87
50	212.76	0.03	0.97	0.06	33.31	0.32	0.97	21.02	95.21	0.83

Temkin < Langmuir < Freundlich. The good fit obtained with the Freundlich model suggests that the adsorption of RB5 on the BMAC may involve multilayer adsorption with interactions between the dye molecules and the heterogeneous nature of the BMAC surface is also implied. The results agreed with the works carried out by previous researchers which reported that the Freundlich model gave a better fit than the Langmuir model on the adsorption of C.I. Reactive Black 5 using surfactant-modified activated carbon [36] high lime soma fly ash [37], cotton plant wastes—stalk (CS) and hull (CH) [10].

4.7. Adsorption kinetics

From the slopes and intercepts of plots of log $(q_e - q_t)$ vs. t obtained at the initial concentrations of 50, 100, 200, 300, 400, and 500 mg/L and at 30°C, first-order rate constant (k_1) and $q_{e1\ cal}$ values were determined. Fig. 4(a) shows a plot of the linearized form of the pseudo-first-order model at all concentrations studied. A comparison of the results with the correlation coefficients and rate constant (k_1) is shown in Table 2. The correlation coefficients for the first-order kinetic model obtained at all the studied concentrations and temperatures were relatively high (R^2 values greater than 0.93) and Δq values ranging from 1.40 to 8.40%.

Using Eq. (8), t/q_t was plotted against t at 50, 100, 200, 300, 400, and 500 mg/L initial dye concentrations and at 30°C, pseudo-second-order adsorption rate constant (k_2) and q_{e2} values were also determined from the slope and intercept of the plots. The plot of the linearized form of the pseudo-second-order model is shown in Fig. 4(b). The values of the parameters k_2 and calculated and experimental q_{e2} and of correlation coefficients are also presented in Table 2. The correlation coefficients for the pseudo-second-order kinetic model were obtained greater than 0.98 for all the concentrations and temperatures studied. Moreover, the experimental $q_{e,exp.}$ values agreed satisfactorily with the calculated values which resulted in Δq values ranging from 0.18 to 3.21%.

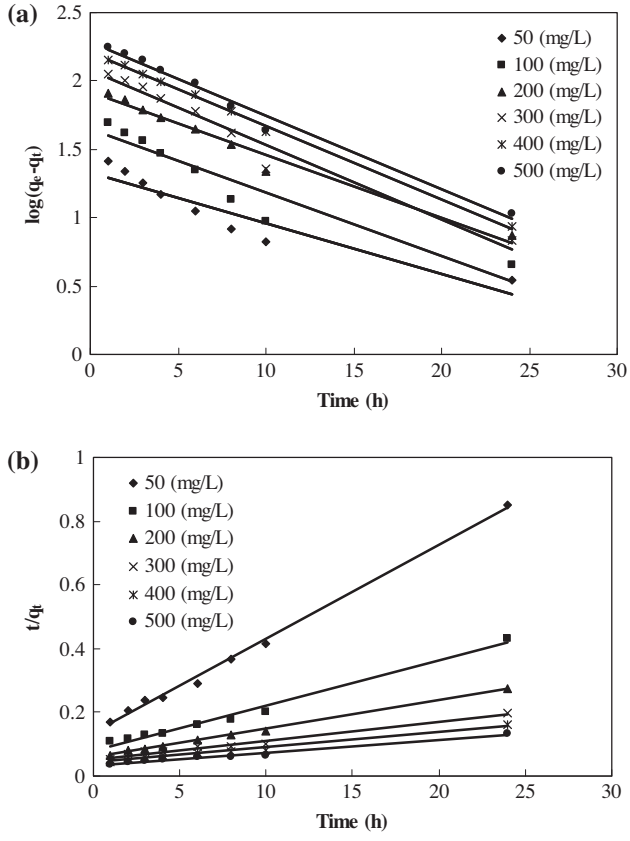

Fig. 4. Adsorption kinetics for adsorption of RB5 on BMAC at 30°C; (a) pseudo-first-order and (b) pseudo-second-order.

From Table 2, it can be observed that the kinetic data were fitted into the pseudo-first-order and pseudo-second-order kinetic models at 30°C. The adsorption kinetics was found to follow closely the pseudo-second-order kinetic model of the RB5 on MBAC at all initial concentrations. The pseudo-second-order kinetic model based on the equilibrium chemical adsorption, that predicts the behavior over the whole range of studies, strongly supports the validity and agrees with chemisorption being rate controlling [21]. This suggested that the overall rate of the adsorption process was controlled by chemisorp-

Table 2
Pseudo-first-order and pseudo-second-order kinetic model parameters for different initial RB5 concentrations at 30°C

C_o (mg/L)	$q_{e,\ exp}$ (mg/g)	Pseudo-first-order kinetic model				Pseudo-second-order kinetic model			
		$q_{e1\ cal}$ (mg/g)	k_1 (h^{-1})	R^2	Δq (%)	$q_{e2\ cal}$ (mg/g)	$k_2 \times 10^{-3}$ (g/mg h)	R^2	Δq (%)
50	31.25	24.24	0.077	0.93	8.40	27.93	4.94	0.98	3.21
100	56.23	53.98	0.130	0.99	1.40	55.86	1.92	0.99	0.18
200	89.34	82.02	0.104	0.98	3.12	86.21	1.29	0.99	1.05
300	118.23	127.61	0.132	0.98	2.91	125.01	0.66	0.98	1.72
400	137.11	140.12	0.140	0.99	2.60	135.13	0.82	0.99	0.43
500	157.54	159.95	0.167	0.98	2.57	147.05	0.98	0.99	2.01

tions which involved valency forces through sharing or exchange of electrons between dye anions and adsorbent, provides the best correlation of the data for the dye [20]. A similar result was reported in the adsorption of C.I. Reactive Black 5 by powdered activated carbon (PAC) [9], and nitric acid-treated bamboo waste for the removal of methylene blue [38].

4.8. Validity of kinetic modeling

Attempt was further made to assess the reasonability of our choice of the pseudo-second-order model as a better fit over the pseudo-first-order model by employing the normalized standard deviation analysis technique. Table 2 shows that the order of Δq (%) was pseudo-second-order < pseudo-first-order in most experimental conditions. This indicates that the pseudo-second-order equation was better in describing the adsorption kinetics of RB5 on BMAC. In addition, the pseudo-second-order rate equation agrees well with experimental data and the linear correlation coefficients are higher than 0.98 for all initial concentrations. Similar phenomena have been observed in the adsorption on coconut shell-based activated carbon [39] and coir pith carbon [40].

4.9. Adsorption mechanism

The intraparticle diffusion model rate constant, k_i is obtained from the slope of the straight line resulting from the plot of q_t vs. $t^{1/2}$ (Fig. 5). The values of the intercept gave an idea about the boundary layer thickness as such that the larger the intercept, the greater is the boundary layer effect [28]. The existence of two separate regions at high initial dye concentrations (more than 300 mg/L), the first stage was near completion within the first 10 h and the second stage where intraparticle diffusion controls immediately followed. The first step in the diffusion model was the mass transfer of adsorbate molecules from

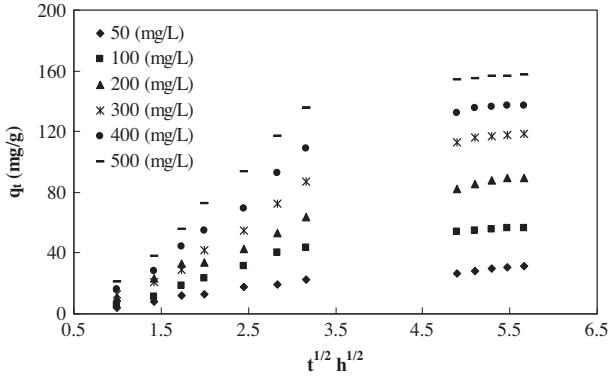

Fig. 5. Intraparticle diffusion kinetics for adsorption of RB5 on BMAC at 30°C.

the bulk solution to the adsorbent surface (the instantaneous stage) and the second stage is the intraparticle diffusion of adsorbate within the on MBAC pore structure. The process of diffusion, mass transfer to the external surface was assumed to be rapid for the adsorption on MBAC. The different stages of rates of adsorption observed indicated that the adsorption rate was initially faster and then slowed down when the time increased. It shows that intraparticle diffusion was not the only rate limiting mechanism in the adsorption process. The values of k_i, C, and correlation coefficient, R^2 obtained for the plots are given in Table 3. The k_i values were found to be generally increased with the increasing RB5 initial concentration which was due to the greater driving force [41].

4.10. Adsorption thermodynamics

The values of ΔH° and ΔS° were calculated from the slope and intercept of Van't Hoff plots of $\ln K_c$ vs. $1/T$ (Fig. 6). The calculated values of ΔH°, ΔS°, and ΔG° are listed in Table 4. The positive value of ΔH°

Table 3
Intraparticle diffusion model constants and correlation coefficients for adsorption of RB5 on BMAC at 30°C

C_o (mg/L)	Intraparticle diffusion model					
	K_{i1} (mg/g h$^{1/2}$)	K_{i2} (mg/g h$^{1/2}$)	C_1	C_2	$(R_1)^2$	$(R_2)^2$
50	5.246	–	2.37	–	0.95	–
100	10.44	–	1.89	–	0.93	–
200	16.28	–	2.31	–	0.97	–
300	34.95	3.62	27.18	80.99	0.98	0.87
400	42.95	6.11	30.14	103.21	0.99	0.79
500	52.73	6.67	35.63	106.94	0.99	0.93

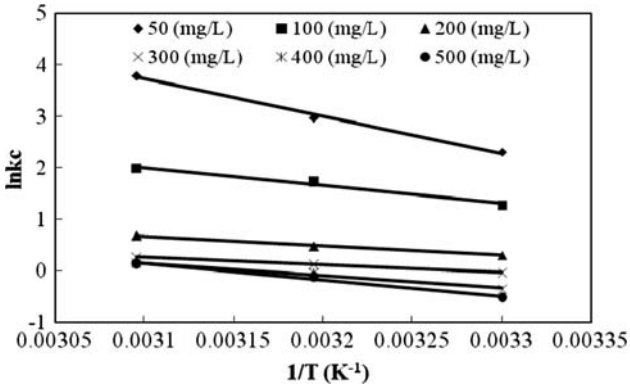

Fig. 6. Plot of $\ln K_c$ vs. $1/T$ at various initial RB5 concentrations.

Table 4
Thermodynamic parameters for adsorption of RB5 on BMAC

Temperatures (°C)	Thermodynamics parameters		
	$-\Delta G^\circ$ (kJ/mol)	ΔH° (kJ/mol)	ΔS° (J/mol K)
30	1.98		
40	1.97	27.33	66.79
50	2.64		

indicated the endothermic. From Table 1, the maximum monolayer adsorption capacity of RB5 onto the prepared activated carbon increased from 169.49 to 212.76 mg/g with an increase in solution temperature from 30 to 50°C. This further confirmed the endothermic nature of the adsorption process. The adsorption reaction for the endothermic processes could be due to the increase in temperature increased the rate of diffusion of the adsorbate molecules across the external boundary layer and in the internal pores of the adsorbent particle, owing to the decrease in the viscosity of the solution [32]. The positive value of ΔS° showed the affinity of the bamboo based activated carbon for RB5 and the increasing randomness at the solid-solution interface during the adsorption process. The negative value of ΔG° indicated the feasibility of the process and the spontaneous nature of the adsorption with a high preference of RB5 onto the prepared activated carbon. Similar observations were reported for adsorption of MB, CV, and RB (ΔH° 19.5, 73.3, 10.7 kJ/mol and ΔS° 75.2, 242.6, 40.7 J/K mol, respectively) onto acidic treatment of activated carbon [32] and adsorption of Amido Black 10B dye onto palm flower activated carbon [42].

5. Conclusion

The BMAC used in this work could substitute for the use of commercial activated carbon as adsorbent due to its availability, high adsorption capacity, and low cost. The results showed that BMAC was a promising adsorbent for the removal of RB5 from aqueous solutions over a wide range of concentrations. Low pH was proved to be more favorable for adsorption of RB5 on the activated carbon. The maximum monolayer adsorption capacities of the MBAC for removal of RB5 was determined from the Langmuir equation and found to be 169.49, 204.08, and 212.76 mg/g at 30, 40, and 50°C, respectively. The equilibrium data were best described by the Freundlich isotherm model. The kinetics of RB5 adsorption followed a pseudo-second-order rate more perfectly. Various thermodynamic parameters such as standard enthalpy (ΔH°), standard entropy (ΔS°), and standard free energy (ΔG°) were evaluated.

Acknowledgments

The authors acknowledge the research grant provided by University Science of Malaysia under the RU Grant Scheme that resulted in this article.

References

[1] S. Aber, N. Daneshvar, S.M. Soroureddin, A. Chabok, K. Asadpour-Zeynali, Study of acid orange 7 removal from aqueous solutions by powdered activated carbon and modeling of experimental results by artificial neural network, Desalination 211 (2007) 87–95.

[2] A.A. Ahmad, B.H. Hameed, Fixed-bed adsorption of reactive azo dye onto granular activated carbon prepared from waste, J. Hazard. Mater. 175 (2010) 298–303.

[3] K.Z. Elwakeela, M. Rekaby, Efficient removal of reactive black 5 from aqueous media using glycidyl methacrylate resin modified with tetraethelenepentamine, J. Hazard. Mater. 188 (2011) 10–18.

[4] S. Papic, N. Koprivanac, A.L. Bozic, A. Metes, Removal of some reactive dyes from synthetic wastewater by combined Al(III) coagulation/carbon adsorption process, Dyes Pigm. 62 (2004) 291–298.

[5] M.S. Tanyildizi, Modeling of adsorption isotherms and kinetics of reactive dye from aqueous solution by peanut hull, Chem. Eng. J. 168 (2011) 1234–1240.

[6] A.A. Ahmad, A. Idris, B.H. Hameed, Color and COD reduction from cotton textile processing wastewater by activated carbon derived from solid waste in column mode, Desalination Water Treat. 41 (2012) 224–231.

[7] A.W.M. Ip, J.P. Barford, G. McKay, A comparative study on the kinetics and mechanisms of removal of reactive black 5 by adsorption onto activated carbons and bone char, Chem. Eng. J. 157 (2010) 434–442.

[8] B.H. Hameed, A.A. Ahmad, N. Aziz, Adsorption of reactive dye on palm-oil industry waste: equilibrium, kinetic and thermodynamic studies, Desalination 247 (2009) 551–560.

[9] A. Hatem, M. AL-Aoha, A.A. Jamil Maaha, M. Ahmadb, Radzi Bin Abas Adsorption of 4-nitrophenol on palm oil fuel ash activated by amino silane coupling agent, Desalination Water Treat. 40 (2012) 159–167.

[10] O. Tunc, H. Tanacı, Z. Aksu, Potential use of cotton plant wastes for the removal of remazol black B reactive dye, J. Hazard. Mater. 163 (2008) 187–198.

[11] B.H. Hameed, A.T.M. Din, A.L. Ahmad, Adsorption of methylene blue onto bamboo-based activated carbon: kinetics and equilibrium studies, J. Hazard. Mater. 141 (2007) 819–825.

[12] M. El-Guendi, Homogeneous surface diffusion model of basic dyestuffs onto natural clay in batch adsorbers, Adsorpt. Sci. Technol. 8(2) (1991) 217–225.

[13] I. Langmuir, Adsorption of gases on plain surfaces of glass mica platinum, J. Am. Chem. Soc. 40 (1918) 136–403.

[14] T.W. Weber, Chakkravorti Pore and diffusion models for fixed-bed adsorption, AIChE J. 20 (1974) 228–238.

[15] H.M.F. Freundlich, Uber die adsorption in losungen, J. Phys. Chem. 57 (1906) 385–470.

[16] F. Haghseresht, G. Lu, Adsorption characteristics of phenolic compounds onto coal-reject-derived adsorbents, Energy Fuels 12 (1998) 1100–1107.

[17] K. Fytianos, E. Voudrias, E. Kokkalis, Sorption–desorption behavior of 2,4-dichloriphenol by marine sediments, Chemosphere 40 (2000) 3–6.

[18] M.J. Temkin, V. Pyzhev, Recent modifications to Langmuir isotherms, Acta Physiochim. USSR 12 (1940) 217–222.

[19] S. Lagergren, About the theory of so-called adsorption of soluble substance, Kung Sven. Veten. Hand. 24 (1898) 1–39.

[20] Y.S. Ho, G. McKay, Sorption of dye from aqueous solution by peat, Chem. Eng. J. 70 (1998) 115–124.

[21] R.L. Tseng, S.K. Tseng, Pore structure and adsorption performance of the KOH-activated carbons prepared from corncob, J. Colloid Interface Sci. 287 (2005) 428–437.

[22] W.J. Weber, J.C. Morriss, Kinetics of adsorption on carbon from solution, J. Sanitary Eng. Div. Am. Soc. Civ. Eng. 89 (1963) 31–60.

[23] K.V. Kumar, A. Kumaran, Removal of methylene blue by mango seed kernel powder, Biochem. Eng. J. 27 (2005) 83–93.

[24] A.A. Ahmad, B.H. Hameed, Effect of preparation conditions of activated carbon from bamboo waste for real textile wastewater, J. Hazard. Mater. 173 (2010) 487–493.

[25] A.A. Ahmad, B.H. Hameed, Reduction of COD and color of dyeing effluent from a cotton textile mill by adsorption onto bamboo-based activated carbon, J. Hazard. Mater. 170 (2009) 612–619.

[26] O. Hamdaoui, E. Naffrechoux, Modeling of adsorption isotherms of phenol and chlorophenols onto granular activated carbon. Part II. Models with more than two parameters, J. Hazard. Mater. 147 (2007) 401–411.

[27] D. Prahas, Y. Kartika, N. Indraswati, S. Ismadji, Activated carbon from jackfruit peel waste by H_3PO_4 chemical activation: pore structure and surface chemistry characterization, Chem. Eng. J. 140 (2008) 32–42.

[28] K. Santhy, P. Selvapathy, Removal of reactive dyes from wastewater by adsorption on coir pith activated carbon, Bioresour. Technol. 97 (2006) 1329–1336.

[29] P.N. Palanisamy, P. Sivakumar, Kinetic and isotherm studies of the adsorption of acid blue 92 using a low-cost non-conventional activated carbon, Desalination 249 (2009) 388–397.

[30] O. Gulnaz, A. Kaya, S. Dincer, The reuse of dried activated sludge for adsorption of reactive dye, J. Hazard. Mater. B134 (2006) 190–196.

[31] S.G. Poulopoulos, M. Nikolaki, D. Karampetsos, C.J. Philippopoulos, Photochemical treatment of 2-chlorophenol aqueous solutions using ultraviolet radiation, hydrogen peroxide and photo-Fenton reaction, J. Hazard. Mater. 153 (2008) 582–587.

[32] S. Wang, Z.H. Zhu, Effects of acidic treatment of activated carbons on dye adsorption, Dyes Pigm. 75 (2007) 306–314.

[33] T. Karthikeyan, S. Rajgopal, L.R. Miranda, Chromium(VI) adsorption from aqueous solution by *Hevea brasilinesis* sawdust activated carbon, J. Hazard. Mater. 124 (2005) 192–199.

[34] S. Senthilkumaar, P. Kalaamani, K. Porkodi, P.R. Varadarajan, C.V. Subburaam, Adsorption of dissolved reactive red dye from aqueous phase onto activated carbon prepared from agricultural waste, Bioresour. Technol. 97 (2006) 1618–1625.

[35] S. Netpradit, P. Thiravetyan, S. Towprayoon, Adsorption of three azo reactive dyes by metal hydroxide sludge: effect of temperature, pH, and electrolytes, J. Colloid Interface Sci. 270 (2004) 255–261.

[36] H.D. Choi, M.C. Shin, D.H. Kim, C.S. Jeon, K. Baek, Removal characteristics of reactive black 5 using surfactant-modified activated carbon, Desalination 223 (2008) 290–298.

[37] Z. Eren, F.N. Acar, Equilibrium and kinetic mechanism for reactive black 5 sorption onto high lime Soma fly ash, J. Hazard. Mater. 143 (2007) 226–232.

[38] B.H. Hameed, I.A.W. Tan, Nitric acid-treated bamboo waste as low-cost adsorbent for removal of cationic dye from aqueous solution, Desalination Water Treat. 21 (2010) 357–363.

[39] M. Radhika, K. Palanivelu, Adsorptive removal of chlorophenols from aqueous solution by low cost adsorbent-kinetics and isotherm analysis, J. Hazard. Mater. B138 (2006) 116–124.

[40] C. Namasivayam, D. Kavitha, Adsorptive removal of 2-chlorophenol by low-cost coir pith carbon, J. Hazard. Mater. B98 (2003) 257–274.

[41] A. Özer, G. Dursun, Removal of methylene blue from aqueous solution by dehydrated wheat bran carbon, J. Hazard. Mater. 146 (2007) 262–269.

[42] S. Nethaji, A. Sivasamy, Adsorptive removal of an acid dye by lignocellulosic waste biomass activated carbon: equilibrium and kinetic studies, Chemosphere 82 (2011) 1367–1372.